ELSEVIER

Contents lists available at ScienceDirect

Sustainable Energy Technologies and Assessments

journal homepage: www.elsevier.com/locate/seta



Original article

Techno-economic analysis for the sunlight-powered reverse water gas shift process: Scenarios, costs, and comparative insights

Cássio Xavier Silva ^a, Jonathan Moncada Botero ^a, Francesc Sastre ^b, Jonathan van den Ham ^b, Pascal Buskens ^{b,c}, Nicole Meulendijks ^b, Remko J. Detz ^{a,*}

- ^a The Netherlands Organisation for Applied Scientific Research (TNO), Energy Transition Studies, Amsterdam, the Netherlands
- b The Netherlands Organisation for Applied Scientific Research (TNO), Materials Solutions, Eindhoven, the Netherlands
- ^c Hasselt University, Institute for Materials Research, Design and Synthesis of Inorganic Materials (DESINe), Diepenbeek, Belgium

ABSTRACT

The deployment of renewable chemicals and fuels production is directly connected to technical developments, political incentives and investments. The route towards market competitiveness of such chemicals and fuels requires significant cost reduction from state-of-the-art production and operation. In this manuscript, we estimate to what extent the expected technical improvements of the sunlight-powered reverse water gas shift process catalysed by a Au/TiO_2 photocatalyst can improve its economic performance. Multiple factors and different scenarios are explored to identify the main dependencies that drive price reductions for this technology. Our projections indicate that the total capital investments required to deploy this green CO production route have the potential to decline from 325 million euros down to 51 million euros for an annual CO production of 100 kton based on the technical improvements. The levelized cost of CO could decrease from around 205 ϵ/GJ CO to 53 ϵ/GJ CO. These results indicate that sunlight-powered chemistry can become competitive when higher carbon taxes are applied to the production of fossil CO (75-200 ϵ/GJ con CO₂).

Introduction

To diminish the effects of the global warming, countries worldwide commit to reducing carbon emissions in accordance with international agreements like the Paris Agreement [1]. These efforts target achieving carbon-neutrality within decades, emphasizing the need to reduce reliance on fossil resources for both energy and industrial use [2]. A pivotal domain for achieving a fossil-free future is CO₂ capture and utilization (CCU) technologies [3]. CCU involves capturing CO₂ from flue gases and/or the atmosphere and utilizing it as feedstock for circular conversion routes. One application involves converting captured CO₂ into synthetic fuels and platform chemicals (e.g. CH₄ and CO) through processes like the Sabatier reaction (Equation (1) and reverse water–gas shift reaction (rWGS, Equation (2) [4 5]. Such approaches decrease industrial dependence on fossil carbon feedstock, enabling the production of essential green chemicals and fuels while conserving fossil resources [6].

$$CO_2 + 4H_2 \rightarrow CH_4 + 2H_2O \Delta H_{298K} = -165.0 \text{ kJ/mol}$$
 (1)

$$CO_2 + H_2 \rightleftharpoons CO + H_2O \Delta H_{298K} = 41.2 \text{ kJ/mol}$$
 (2)

Various CCU technologies are explored for CO₂ conversion to CO or CH₄,

including approaches driven by electrical or thermal energy [7 8 9 10 11]. Photocatalytic technologies use directly the (sun)light as a sustainable energy source that combined with a photocatalysts promote the reaction [11 12 13 14 15 16]. Furthermore, there has been significant recent progress in the extensive study of general solar-driven CO2 reduction to CO and CH₄ documented in the literature [17]. Further potential advantages of photocatalytic conversion technologies include (i) high energy efficiency with minimized conversion and transportation losses, (ii) high process selectivity with minimized need for energy and cost intensive downstream processing, (iii) ease of scaling up and down (numbering up) making a good fit with small, medium and large sized CO2 sources, (iv) steep learning curves and fast cost reductions expected based on technology modularity, (v) decentralized and potentially offgrid production, and (vi) low carbon footprint for direct use of sunlight. An example of such a process is the light-driven plasmon-enhanced photocatalytic conversion of CO₂ and H₂ to produce CH₄ or CO [11 12 17 13 19]. Metallic plasmonic nanoparticles attached to a metal oxide material are used as catalysts to enhance sunlight utilization [13 9 19

In previous work, we analysed the techno-economic prospects for the light-driven Sabatier process, concluding that the methanation process could compete with natural gas by 2050 [20 21]. In addition, a steady-

E-mail address: remko.detz@tno.nl (R.J. Detz).

^{*} Corresponding author.

state modelling study combining Sabatier and rWGS has recently been published by Li et al. [22]. In contrast, in this work, we delve into the rWGS process, providing a comprehensive analysis of the complete reaction system and exploring various parameters that influence the cost dynamics. Because of the endothermicity of the rWGS reaction, light is not only used to overcome the activation energy barrier but its energy is also (partially) stored in the CO molecule, thereby storing solar energy in chemicals. The rWGS photocatalysis technology has already been demonstrated in the lab [13 18 23] and pilot studies in relevant environment are underway [24 25]. Conducting a techno-economic analysis in the early stages of technology development is an important step to identify potential cost-saving measures, highlight key design parameters, and provide insights into the market potential of the technology. By identifying potential challenges early on, developers can make better substantiated decisions and optimize the technology to reduce costs and increase efficiency during the scale-up process.

Herein, we report a technoeconomic analysis for the solar powered rWGS process. The cost projection analysis has been stablished by defining the experimental base, the initial solar powered rWGS system design and its costs. This involves identifying main parameters, inputs and outputs. We then assessed a scaled-up photochemical plant with optimized process performance. Subsequently, we have conducted a bottom-up investment cost analysis to determine total system cost. The economic feasibility of the photocatalytic rWGS process involves a levelized CO production cost analysis. The production costs are compared to those of incumbent technology. Sensitivity analysis explores the dependency of the production costs on parameters such as capacity, feedstock price, and energy costs, identifying technical bottlenecks and guiding directions for improvement. The analysis of the different parameters and the costs provides a valuable perspective on the future research direction that can guide to scale-up this process.

Experimental basis for photocatalytic CO production

Industrial solar powered photocatalytic systems to produce CO are not yet available, but previous research indicates that plasmoic production of CO can be achieved by using a Au/TiO2 catalyst without external heating [13]. The photocatalytic system is deposited in a platelike reactor (visual representation of the reactor system in Figure S1-Supporting Information (SI)) with an Au loading of 3.1 wt%. The CO production rate was assessed under mild solar light concentrations (6 to 14 kW.m⁻²) and catalyst loadings (127 to 1115 g.m⁻²) under a consistent CO₂ and H₂ input flow. Additionally, the optimal CO₂:H₂ molar ratio was optimized to maximize CO output. It is essential to highlight that, to conduct the experiments while avoiding any interference from mass transfer in the measurements, a high input stream of $3.6 \, l.h^{-1}$ of H_2 and CO_2 was used, flowing through a disc of 625×10^{-6} m² of area. This results in a flow of $1.3 \times 104 \text{ l.h}^{-1}$.m², and consequently in a deliberately low conversion rate of CO₂ (below 1 % of experimental yield). The intentionally increased input flow in the experimental setup aimed to minimize the yield artificially, ensuring accurate CO production measurement and mitigating potential inaccuracies due to mass transfer limitations. As a result, the reported yield of approximately 1 % does not represent a realistic yield under normal operating conditions. Temperature measurements were also conducted across the various solar concentrations (from 6 to 14 suns) and reveal a temperature range of 80–150 °C. This range exhibited a linear increase versus an increasing solar concentration [13]. Additionally, temperature measurements revealed a significant temperature gradient within the illuminated catalyst bed, with a potential temperature difference of up to 150 °C between the surface temperature measured and the actual temperature within the catalyst bed [26]. This temperature variance influences reaction kinetics and catalyst stability, underscoring the critical role of temperature in photo-thermal driven rWGS processes, as reported in various literature [9 12 17].

The study reported several key findings. Firstly, the laboratory

process achieved an apparent quantum efficiency (AQE) of 4.15 % (number of reacted electrons forming CO in comparison to the number of incident photons) [13]. Secondly, the CO production rate increases exponentially when the solar light concentration was enhanced linearly. This relationship has been corroborated by previous studies [13 19 18] and conforms to the Arrhenius equation. Finally, a linear increase of the catalyst weight did not lead to a linear increase of the CO production rate, as an inhibitory shielding effect occurred, resulting in a partly inactive catalyst. This occurs because when thicker layers of catalyst loading are present, light cannot penetrate to the lowest part of the catalyst bed, causing that portion to remain unreacted. A catalyst loading of 0.22 kg.m⁻² resulted in the most CO produced per amount of catalyst, while loadings between 0.13 and 0.64 kg.m⁻² were tested. Finally, the study concluded that the highest CO production rate of 7.4 mol·m⁻²·h⁻¹, achieved with a 0.22 kg.m⁻² catalyst loading, was attained at a CO₂:H₂ ratio of 4:1 at 14 kW.m⁻². These experimental results act as the starting point for this techno-economic analysis.

Formulating scenarios for the scaled-up production

The experimental setup is not suitable for large scale operation and, to analyse the economic feasibility of the route, we formulate two scenarios in which the technology has been optimized for industrial implementation. These two scenarios are based on data that are derived from the experimentally observed trends. The experiments indicate that the CO production rises exponentially for an increase in irradiation (SI, Figure S2). This trend is extrapolated to vary the irradiation and $\rm CO_2$ conversion yield, influencing input flow, production, and efficiency, as presented in Table 1.

The scenarios are outlined below:

- Experimental scenario: encompassing original experimental configurations, it features 14 kW.m⁻² irradiation, <1% yield, 7.4 mol.m⁻².
 h⁻¹ production rate, and 4 % of energy efficiency.
- Base scenario: retains primary parameters, assuming 10 % yield through reduced input flow. Includes 14 kW.m⁻² irradiation, 10 % yield (expected realistic conversion rate), 7.4 mol.m⁻². h⁻¹ CO production rate, and 4 % of energy efficiency.
- Developed scenario: Considers extrapolation results for a higher sun concentration [13] with maximum equilibrium yield. Parameters: 25 kW.m⁻² irradiation, 18 % yield (based on Li, S. et al. equilibrium conversion rate [22]), 148 mol.m⁻². h⁻¹ CO production rate, 46 % of energy efficiency.

The techno-economic analysis focuses on the base and developed scenarios, as they are most suitable for practical application.

Designing a photochemical plant for CO production

We establish a preliminary system configuration of a photochemical plant to produce 100 ktons (or $10\,\mathrm{PJ}$) of CO output per year, as presented in Fig. 1. Sunlight is used as sole energy source for the reaction, and some of the generated heat is recovered after the reaction, at an assumed pressure of 20 bar, while the input flows of green CO_2 and H_2 input are

CO production parameters for the different scenarios created from the experimental results.

	Experim.	Base	Developed
Irradiation (kW.m ⁻²)	14	14	25
Yield (CO out/CO _{2 in})	0.9 % ^a	10 %	18 %
Input Flow (mol.m ⁻² .h ⁻¹)	1025	93	1025
Production (mol.m $^{-2}$. h $^{-1}$)	7.4	7.4	148
Efficiency (J _{CO out} /J _{LIGHT in})	4 %	4 %	46 %

^a The experimental yield was deliberately kept low by implementing an excessive input flow. This was done to enhance the accuracy of CO production measurements.

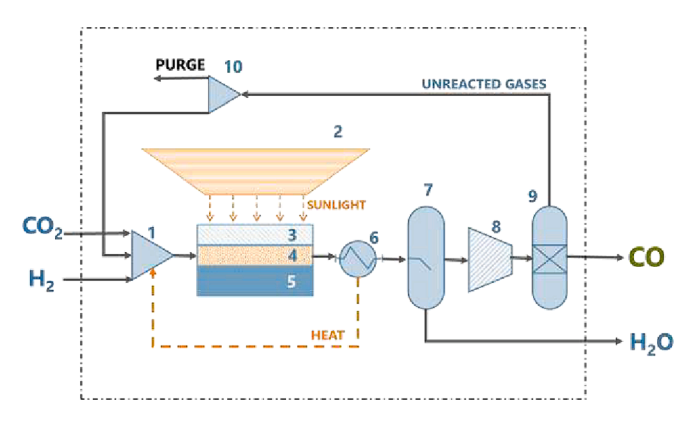


Fig. 1. Schematic representation of the system configuration of a 100 kton photocatalytic CO production process. The different components (1–11) are discussed in the text.

considered to be pressurized (20–70 bar pressure of CO_2 and H_2 [27]). The mass and energy balance of the reaction can be found on the supporting information (SI, Figure S3).

The system includes a mixer unit (1) to receive and mix the CO_2 and H_2 input streams in a 4:1 ratio; a light concentrator (2) to increase sunlight power to 14–25 kW.m $^{-2}$ at the reactor surface. The photoreactor features a transparent window (3) allowing sunlight penetration into the reaction chamber (4), where the Au/TiO_2 catalyst is connected to the inlet streams of reactive gases. A support structure (5) with a metal isolated base offers structural stability to the photoreactor components. After the reaction, the output flows through a heat exchanger (6) to adjust the temperature and recover some of the heat generated. Subsequently, a water separation unit (7) removes water from the output stream before the compressor (8) that adjusts the pressure to 20 bar before entering the separation unit – pressure swing adsorption (PSA) unit (9), where CO is separated from the excess H_2 and CO_2 . The primary product, green CO_2 is ready for follow-up chemistry or can be pressurized and transported – these stages were not analysed in this study.

To optimize carbon conversion efficiency in a larger industrial system, unreacted CO_2 and H_2 are separated and recycled back into the photoreactor, ensuring maximal CO_2 utilization, promoting sustainability, and likely cost-effectiveness. The reaction also displays a selectivity of 97 % for CO and 3 % for CH_4 formation. To simplify the system configuration and economic evaluation, the remaining CH_4 formed in the recycle stream is separated and purged through a splitter (10). In practical operation, this remaining CH_4 could be utilized to power the facility or serve as a product, enhancing the systems efficiency. For both scenarios described in the previous section, the configuration remains virtually the same. However, higher irradiation levels result in increased heat generation within the reactor. This improves the reaction rate but also necessitates larger cooling capacities afterwards to maintain optimal operating conditions. We have taken this into account in our cost estimations.

Investment cost analysis

To estimate the photochemical plant cost, the main components have been divided into three categories: the light concentrator, the photoreactor, and the auxiliary equipment. The costs of the entire process, depicted in Fig. 1, are further categorized into equipment costs, direct costs, and indirect costs. For the light concentrator system, we adopt the total cost assumption (equipment, direct, and indirect costs) from NREL's SunRing heliostat designs, which amounts to 96 s/m^2 of concentrator [28]. The photoreactor equipment costs are determined by the individual costs of its main materials: the glass plate, the catalyst (Au), and the support structure (components 3, 4, and 5 - Fig. 1). Among

these, the Au material dominates the investment costs, with a catalyst loading of 3.1 wt% Au amounting to approximately $390 \, {\rm €/m^2}$ of reactor [29 30]. In contrast, the costs for glass and support structure are significantly lower, fixed at nearly $25 \, {\rm €/m^2}$ of reactor. Additionally, other direct and indirect costs, such as installation, instrumentation, electrical systems, engineering, legal expenses, etc., are included as a percentage on top of the equipment cost, utilizing specific factors that are provided in the supporting information (see Table S1 - SI) – important to note that the factors used for each equipment are not the same [28 31].

Next, we evaluate the costs of all auxiliary equipment (e.g., compressors, heat exchangers, and purification systems) using ASPEN Plus modelling. This analysis directly provides an estimate of the electricity demand for the entire process in the production of 100 kton of CO annually. The direct and indirect costs for the auxiliary equipment are also incorporated as a percentage on top of the equipment cost, using the same factors mentioned previously (see Table S1 - SI). CAPEX is determined for a theoretical plant that operates for 8000 h per year. Correction factors will be applied further to compensate for the sunlight hours.

Further explanation on the calculate steps for the equipment cost and CAPEX can be found on the Supporting Information, while the results for the two selected scenarios are presented in Fig. 2. Investment costs for the base scenario amount to 325 M€, while for the developed case CAPEX reduces significantly to around 51 M€. This reduction can be attributed to a higher CO yield and flow rate per m² of reactor. As a consequence, all components required to produce 100 kton of CO can be downsized. A smaller area of photoreactors can be utilized thanks to the enhanced CO production rate, leading to reduced catalyst needs. For the base case, for instance, the surface area of the photoreactor would be of 0.06 km², while in the developed case this reduces to around 0.003 km². Similarly, a smaller area of sun concentrator is sufficient, as the light-to-CO conversion efficiency improves, while in the base case 1 km2 of concentrators would be needed, in the developed case only 0.1 km² would be necessary. Additionally, the higher yield results in reduced flows of recirculating gases, leading to cost reductions in the most

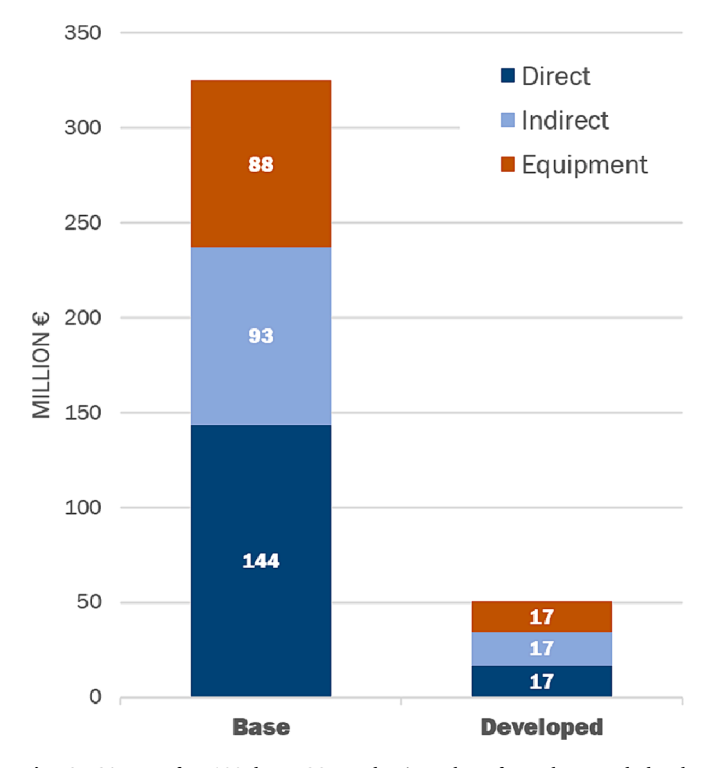


Fig. 2. CAPEX of a 100 kton CO production plant for a base and developed scenario.

expensive auxiliary equipment, such as the compressor and the PSI separation unit.

It's important to recognize that due to the early stage of technology development, there is some uncertainty in our analysis. However, this study offers valuable insights into the potential of sunlight-powered photochemical CO production. The fact that this technology is in its early stages means there's great room for improvement through optimization and system design enhancements (see also Conclusions and recommendations section) suggesting a promising future ahead.

Levelized CO production costs

The levelized cost of CO production (LCoCO) are determined through an annualized cost calculation according to equation (3) [32]. The total annual costs include the discounted annualized CAPEX ($a \times CAPEX$), the fixed O&M costs (O&M), and the annual feedstock costs for green electricity, hydrogen and CO₂ (F). These annual costs are divided by the total annual production of CO (P_{CO}). The capital recovery factor (a) is calculated through equation (4) that depends on the chosen discount rate (r) and the plant lifetime (n) in years.

$$C_{CO} = \frac{(\alpha x CAPEX) + O\&M + F}{P_{CO}} \tag{3}$$

$$\alpha = \frac{r}{1 - (1 + r)^{-n}} \tag{4}$$

For this analysis, we used a discount rate (the interest rate to determine the present value of future cash flows) of 10 %. The general values for lifetime plants in the chemical industry are between 15 and 30 years [33]. The operational or full load hours (FLH) of the plant are directly affected by the amount of sun hours (S_h), since the system only works when there is sunlight, which largely depends on the location. For that reason, the real FLH of the production plant are less than the theoretical FLH presented in the CAPEX analysis, as shown in Table 2.

Our analysis was primarily based on an installation in Andalusia, southeast Spain, renowned for its direct irradiation of 2100 kWh.m $^{-2}$. yr $^{-1}[34]$. Considering the average sun irradiation as 1 kW.m $^{-2}$, this location would typically experience approximately 2100 h per year of direct peak sunlight. The FLH values presented in the baseline LCoCO are tailored to this specific location, with values in parentheses indicating load hours for alternative locations such as the Netherlands (1100 h) and the Sahara desert (2700 h) [34]. For that reason, the CAPEX used for the LCoCO analysis (CAPEX_{REAL}) considers the specific CAPEX costs (CAPEX_{8000h}) divided by an operation factor (Fo), as presented in Equation (5). The operation factor is derived from equation (6).

$$CAPEX_{REAL} = \frac{CAPEX_{8000h}}{F_O} \tag{5}$$

$$F_{O} = \frac{S_{h}}{8000} \tag{6}$$

The O&M costs amount to 3 % of the initial CAPEX. The price for which green CO_2 , H_2 and electricity are available for the plant are

Table 2 Parameters for the LCoCO analysis.

Parameter	Values ^a
CO ₂ (€/kg) [21]	0.02 [0.01-0.60]
H ₂ (€/kg) [21]	4 [1.4–7]
Electricity (€/MWh) [21]	60 [15–100]
O&M (%)	3 % [2–5 %]
FLH (h) [34]	2100 [1100–2700]
Discount (%)[21]	10 % [8–12 %]
Lifetime (years) [33]	25 [10–30]

a ranges used for sensitivity analysis are displayed between brackets.

indicated in Table 2, similar to the values used for CH_4 . The CO_2 , renewable H_2 and electricity costs were taken from the study of B. v. d. Zwaan et al. [21]. The range inside the brackets is used to determine a more optimistic and conservative production costs range and serves as input for our sensitivity analysis. The prices of these commodities are also considered to change in the coming years.

Fig. 3 illustrates the outcome of the LCoCO analysis for the base and developed scenarios, delineating the influence of each cost component on the overall costs. In the base scenario, the annualized CAPEX emerges as the predominant cost contributor, while CO2 and hydrogen contribute to a lesser extent within the levelized cost structure. Total LCoCO for the base scenario amount to 205 €/GJ, while for the developed scenario costs decrease to 53 €/GJ. In the LCoCO of the latter scenario, the OPEX components have a higher contribution, with hydrogen becoming the primary cost element of the production process. It is important to note that these scenarios are constructed based on the current H2 and CO2 prices, the main values indicated in Table 2. It is foreseeable that these prices will change in the future, particularly with the anticipated elevation of CO2 prices due to growing demand as a valuable commodity, and the simultaneous reduction in green hydrogen costs thanks to an increased deployment of green electricity supply and electrolyzer plants.

To capture part of the uncertainties in the cost assessment, a full range of CO production costs is depicted in Fig. 4. The dark blue line aligns with the main parameters of Table 2 and consequently results in the same LCoCO for the two scenarios as depicted in Fig. 3. On the other hand, the light blue area demonstrates LCoCO extremes under different H₂, CO₂, and electricity costs, with the most optimistic scenario depicted as the lower range and the most conservative as the upper range - corresponding to the parameters in Table 2 enclosed in brackets. This range illustrates that under conservative conditions, the LCoCO may become as high as 400 ℓ /GJ, while our most optimistic projection results in a LCoCO of around 30 ℓ /GJ.

The LCoCO of our green photochemical process is also compared to conventional fossil-based CO production costs in Fig. 4. Presently, CO is

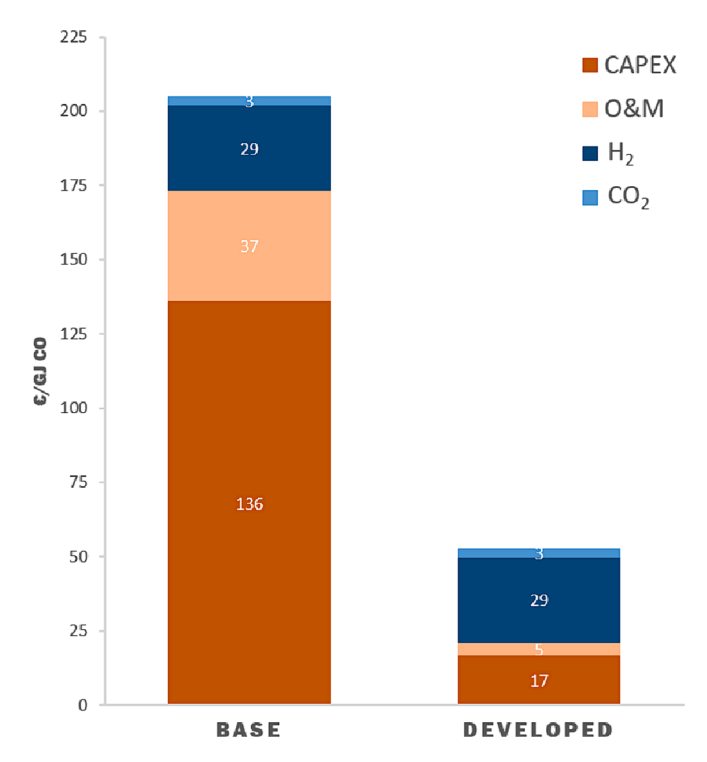


Fig. 3. Breakdown of the LCoCO for the photochemical CO production scenarios. Electricity cost contribution is relatively small and thus not visible at this scale.

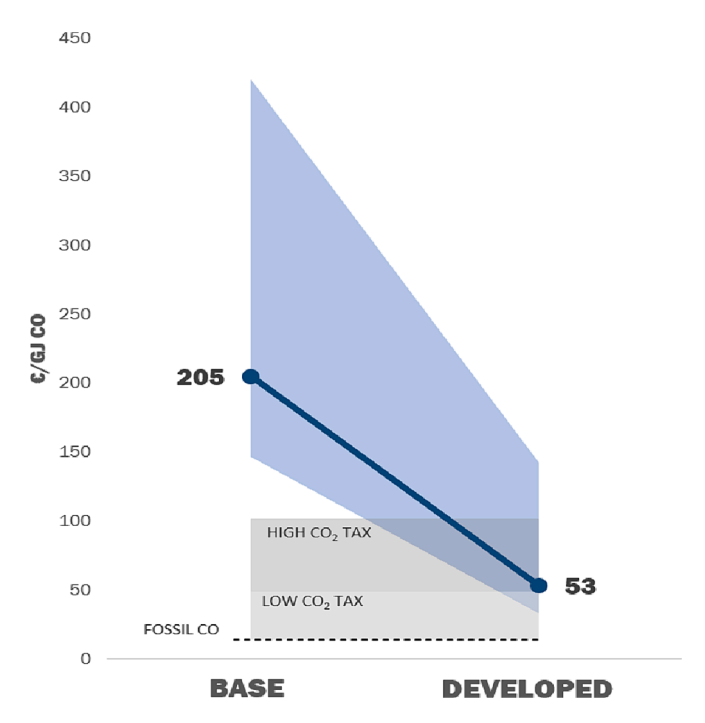


Fig. 4. Projection of CO production costs through photochemical conversion.

predominantly used as a chemical intermediate, particularly in methanol production using syngas derived from natural gas reforming. Our estimation places conventional CO production costs between the market prices of natural gas and methanol [5]. In 2021, European natural gas prices averaged $16~\epsilon/\text{GJ}$ [35], while methanol prices varied between 14 and $32~\epsilon/\text{GJ}$ [36]. After adjusting for CO content in syngas, we approximate conventional CO production costs at $17~\epsilon/\text{GJ}$, without considering purification expenses for CO separation from syngas. Despite slight deviations from other estimates [5 35], these fossil-based CO costs are an order of magnitude lower than the LCoCO of our photochemical process in the base scenario. Also for our developed scenario, the LCoCO is around three times higher than fossil-based CO production costs.

Fossil-based CO costs are profoundly impacted by natural gas prices, which are susceptible to geopolitical tensions, elevated demand, and sustainability measures like CO2 taxation and regulations. We also indicate fossil CO production costs when a CO2 tax is included, considering a low CO2 tax from 0 to 75 €/ton of CO2 and a higher CO2 tax between 75 and 200€/ton of CO2. It is important to notice that the carbon price on the European ETS system already surpassed 100 €/ton of CO2 in 2023, so our "high" carbon tax scenario seems reasonable [38]. Fossil-based syngas production has a carbon emission intensity of 2.5 kg CO₂/kg CO for pyrolysis of heavy fuel oil [37], 2.7 kgCO₂/kg CO for auto-thermal reforming process (ATR) and up to 4.2 kg CO₂/kg CO for steam methane reforming (SMR) [37]. Those numbers include upstream and downstream emissions of CO2eq, considering that the CO produced is combusted. In these scenarios, plasmonic assisted rWGS is expected to become competitive versus fossil-based CO production, in case that CO2 taxes are applied (Fig. 4). The technology will become more profitable with in the developed scenario and if the willingness to pay for a renewable CO alternative increases and/or fossil fuel prices rise.

Sensitivity analysis

We performed a sensitivity analysis for the LCoCO on seven different parameters to identify the key factors that can influence it for the base and the developed case. Among these parameters, the operational hours of the process are mainly determined by the hours of sunlight and have the most substantial impact on the levelized costs of CO in the base

scenario (Fig. 5A). Locations with more hours of sun experience a lower LCoCO of approximately 150 ϵ /GJ, while at more Northern altitudes, the LCoCO doubles. However, in the developed scenario (Fig. 5B), the effect is less extreme because of the larger efficiency, enabling more CO production with less sunlight, reducing the dependency on sun hours to some extent.

In the developed scenario, feedstock costs (H₂ and CO₂) significantly influence production costs, whereas their impact is smaller in the base scenario. However, upon analysing these components separately, it becomes evident that the future cost of CO₂ could drive production costs up substantially. In remote locations where direct air capture could be the only viable CO₂ source, CO₂ costs may amount to 0.60 €/kg [39]. In that case, production costs may rise by as much as 50 % in the base scenario and even more than double in the developed scenario. Similarly, hydrogen prices exert a strong influence on the costs of the developed scenario, potentially lowering costs by up to 30 % for a H₂ price of 1.4 €/kg.

The catalyst cost is driven by the metal (Au) loading. To reduce CAPEX costs of the photoreactor, one possible approach is to reduce the amount of gold in the catalyst or replace it by other metals-as-catalysis (e.g. Cu). In the base scenario, where a substantial portion of the CAPEX comes from the catalyst, this change would have a more significant impact. However, for the developed scenario, which utilizes much less catalyst based on the assumptions made, the difference would be minimal. Besides, the plant lifetime should be at least 20 years. Longer lifetimes do not considerably improve the LCoCO, but costs increase significantly for shorter lifetimes. O&M costs and the discount rate are relative factors to the CAPEX, and as investment costs are the most significant cost component, especially in the base scenario, their impact increases with higher CAPEX values. Overall, it's evident that increasing production efficiency reduces dependency on capital expenditure (CAPEX) components like gold concentration, plant lifetime, and discount rate.

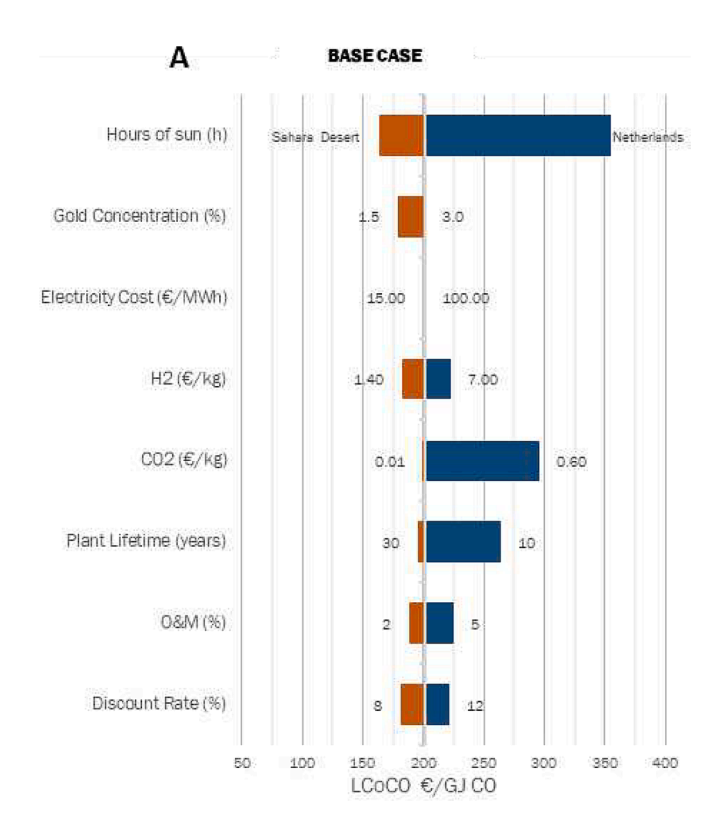


Fig. 5A. LCoCO sensitivity analysis for the base scenario.

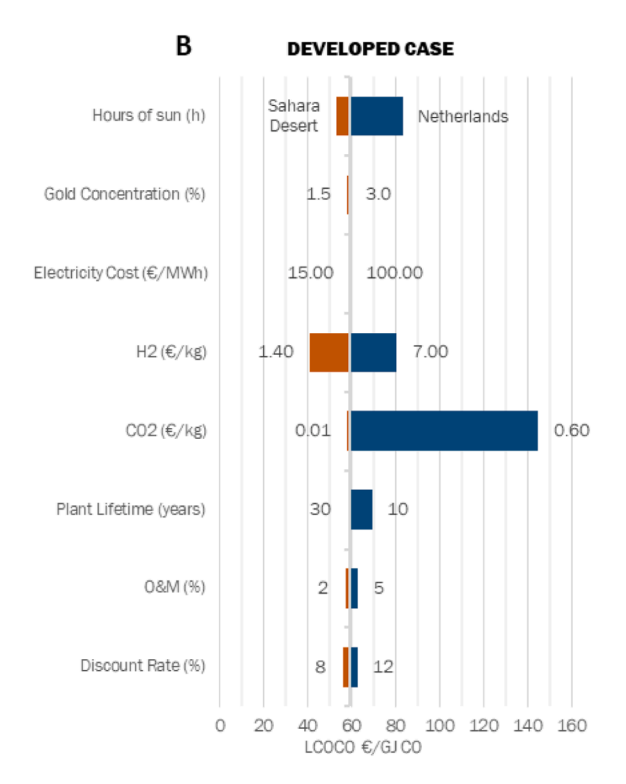


Fig. 5B. LCoCO sensitivity analysis for the developed scenario.

Conclusions and recommendations

The techno-economics of the sunlight-powered photochemical rWGS process, which is catalysed by $\mathrm{Au/TiO_2}$ in a transparent flow reactor, are studied. The process can become a competitive solution for producing CO as renewable carbon feedstock. However, to reach this competitive level with fossil CO, photocatalytic production relies on a combination of technical, political and operational factors.

In the analysis of investment costs, we conducted a bottom-up assessment of the main equipment components: the photoreactor, solar concentrator system, and auxiliary equipment. The contribution of each component's costs varies based on reaction efficiency and the considered light concentration. In our system design, the light concentrator incurs the highest costs, accounting for 56 % of the total CAPEX in the base scenario and 54 % in the developed scenario. The photoreactor costs make up 30 % of the CAPEX in the base scenario and are reduced to 10 % in the developed scenario. Meanwhile, the auxiliary equipment represents 14 % of the CAPEX in the base scenario and increases to 36 % in the developed scenario. The auxiliary equipment costs can be reduced substantially by economies-of-scale effects. A system in which multiple photoreactors (numbering up principle) are connected to a large gas treatment and purification system seems most cost effective. By leveraging higher CO production with enhanced sun concentration and conversion efficiency, total CAPEX for a 100 kton CO production capacity can drop from 325 M€ to 32 M€.

We have also conducted a levelized cost analysis for two selected scenarios. The results suggest that achieving cost parity with the fossil-based benchmark relies on a sufficiently reasonable CO_2 emission pricing, likely somewhere between 75 and $200~\rm fcCO_2$. To realize this scenario, both process throughput and yield need enhancement, as estimated in our study, and the costs of primary feedstocks, CO_2 and H_2 , should align with projected price levels. These operational variables significantly influence pricing when CAPEX reduces, but their impact is contingent on future market dynamics and the progress of unrelated technologies beyond the scope of this study. Nevertheless, price projections indicate that even with anticipated higher operational costs, the

technology could maintain competitiveness against the fossil benchmark. A comprehensive assessment could further explore a comparative analysis of photochemical CO production and alternative green CO production pathways.

Our analysis has identified several key areas that require development to improve the competitiveness of this technology. Firstly, we recommend that research efforts are directed towards enhancing the production rate and yield of the photochemical CO production process, as this would lead to a significant reduction in production costs and increase the feasibility of this technology for widespread implementation. Additionally, exploring alternative process configurations that incorporate the use of artificial light to increase the number of full load hours represents a promising avenue and is currently ongoing. While the impact of increased irradiation on temperature and catalytic efficiency is acknowledged, specific studies on the efficiency and lifetime of the catalyst under these conditions are not available as far as we know. Furthermore, we emphasize the importance of considering a realistic yearly cycle of sunlight-based operation and the associated start-up and shut-down procedures, as well as managing the recycle stream during transient periods. Pursuing these areas of research and development could greatly enhance the competitive potential of this technology for various industrial applications.

CRediT authorship contribution statement

Cássio Xavier Silva: Writing – original draft, Visualization, Methodology, Investigation, Formal analysis, Data curation. Jonathan Moncada Botero: Writing – review & editing, Methodology, Formal analysis, Data curation. Francesc Sastre: Writing – review & editing, Validation, Data curation. Jonathan van den Ham: Writing – review & editing, Validation, Data curation. Pascal Buskens: Writing – review & editing, Validation, Supervision, Funding acquisition, Conceptualization. Nicole Meulendijks: Writing – review & editing, Project administration, Funding acquisition, Conceptualization. Remko J. Detz: Writing – review & editing, Methodology, Investigation, Validation, Supervision, Funding Acquisition, Conceptualization..

Declaration of competing interest

The authors declare that they have no known competing financial interests or personal relationships that could have appeared to influence the work reported in this paper.

Data availability

Data will be made available on request.

Acknowledgements

Part of the research leading up to this paper has been performed in the context of the Interreg project LUMEN ("Sunlight as Fuel for Sustainable Chemical Processes"). We acknowledge financial support for LUMEN from the European Fund for Regional Development of the European Commission through the cross-border collaborative Interreg V program Flanders—The Netherlands (see https://www.project-lumen.com). We would like to thank the LUMEN consortium members for their valuable feedback. Additionally, we acknowledge the contributions of the H2020 Spotlight project, an initiative of the Photonics Public Private Partnership (Grant no. 722788, https://spotlight-project.eu/) for its members valuable inputs for this study.

Appendix A. Supplementary data

Supplementary data to this article can be found online at https://doi.org/10.1016/j.seta.2024.103768.

References

- [1] IEA. The IEA at COP26. Paris: IEA; 2021.
- [2] Olfe-Kräutlein B. Advancing CCU technologies pursuant to the SDGs: a challenge for policy making, Policy Pract. Rev. 2020;8.
- [3] IEA. Carbon Capture, Utilisation and Storage. Paris: IEA; 2022.
- [4] Hernández S, Farkhondehfal MA, Sastre F, Makkee M, Saraccob G, Russoa N. Syngas production from electrochemical reduction of CO2: current status and prospective implementation. Green Chemistry 2017;19:2326–46.
- [5] Detz R, Zwaan BVD. Cost projections for microwave plasma CO production using renewable. J. Energy Chem. 2022;71:507–5013.
- [6] GSTC, "Methanol," Global Syngas technology Council, 2021. [Online]. Available: https://globalsyngas.org/syngas-technology/syngas-applications/chemicals/methanol/. [Accessed 2023].
- [7] Mustafa A, Lougou BG, Shuai Y, Razzaq S, Wang Z, Shagdar E, Zhao J. A technoeconomic study of commercial electrochemical CO2 reduction into diesel fuel and formic acid. J. Electrochem. Sci. Technol. 2021;13(1):148–58.
- [8] Pérez-Gallent E, Turk S, Latsuzbaia R, Bhardwaj R, Anastasopol A, Sastre-Calabuig F, et al. Electroreduction of CO2 to CO paired with 1,2-propanediol oxidation to lactic acid. Toward an economically feasible system. Ind. Eng. Chem 2019;58:6195–202.
- [9] X. Meng, L. Liu, S. Ouyang, H. Xu, D. Wang, N. Zhao and J. Ye, Nanometals for solar-to-chemical energy conversion: from semiconductor-based photocatalysis to plasmon-mediated photocatalysis and photo-thermocatalysis, 2016.
- [10] Sastre F, Muñoz-Batista MJ, Kubacka A, Fernández-García M, Smith WA, Kapteijn F, et al. Efficient electrochemical production of syngas from CO2 and H2O by using a nanostructured Ag/g-C3N4 catalyst. ChemElectroChem 2016;3(9): 1497–502.
- [11] Sastre F, Corma A, García H. 185 nm photoreduction of CO2 to methane by water. Influence of the presence of a basic catalyst. J. Am. Chem. Soc. 2012;134(34): 14137–41.
- [12] Sastre F, Versluis C, Meulendijks N, Rodríguez-Fernández J, Sweelssen J, Elen K, et al. "Sunlight-fueled, low-temperature Ru-catalyzed conversion of CO2 and H2 to CH4 with a high photon-to-methane efficiency. ACS Omega 2019;4(4):7369–77.
- [13] Molina PM, Bossers KW, Detz RJ, Wienk JD, Meulendijks N, Verheijen MA, et al. Sunlight powered continuous flow reverse water gas shift process using a plasmonic Au/TiO2 nanocatalyst. Chem. Asia 2023;18(14):e202300405.
- [14] Corma A, Garcia H. Photocatalytic reduction of CO2 for fuel production: Possibilities and challenges. J. Catal. 2013;308:168–75.
- [15] Neaţu Ş, Maciá-Agulló JA, Garcia H. Solar light photocatalytic CO2 reduction: General considerations and selected bench-mark photocatalysts. Mol. Sci. 2014;15 (4):5246-62.
- [16] Li Y, Lei Y, Li D, Liu A, Zheng Z, Liu H, et al. Recent progress on photocatalytic CO2 conversion reactions over plasmonic metal-based catalysts. ACS Catalysis 2023;13 (15):10177–204.
- [17] Schuurmans JHA, Masson TM, Zondag SDA, Buskens P, Noël T. Solar-Driven continuous CO2 reduction to CO and CH4 using heterogeneous photothermal catalysts: recent progress and remaining challenges. ChemSusChem 2023;17(4). https://doi.org/10.1002/cssc.202301405. Wiley.
- [18] Molina PM, Meulendijks N, Xu DM, Verheijen DMA, Hartog DTd, Buskens PP, Sastre DF. Low temperature sunlight-powered reduction of CO2 to CO using a plasmonic Au/TiO2 nanocatalyst. ChemCatChem 2021;13(21):4507–13.
- [19] Volders J, Elen K, Raes A, Ninakanti R, Kelchtermans A-S, Sastre F, et al. Sunlight-powered reverse water gas shift reaction catalysed by plasmonic Au/TiO2

- nanocatalysts: effects of au particle size on the activity and selectivity. Nanomaterials 2022;12(23):4153.
- [20] Rohlfs J, Bossers KW, Meulendijks N, Mackenzie FV, Xu M, Verheijen MA, et al. Continuous-flow sunlight-powered CO2 methanation catalyzed by γ-Al2O3supported plasmonic Ru nanorods. Catalysts 2022.
- [21] Zwaan BVD, Detz R, Meulendijks N, Buskensd P. Renewable natural gas as climateneutral energy carrier? Fuel 2022.
- [22] Li S, Haussener S. Design and operational guidelines of solar-driven catalytic conversion of CO2 and H2 to fuels. Appl. Energy 2023;33(120617):120617.
- [23] Aniruddha A, Upadhye IR, Zeng X, Kim HJ, Isabel T, A. M. A, Dumesica JA, Huber G. Plasmon-enhanced reverse water gas shift reaction over oxide supported Au catalysts. Catal. Sci. Technol. 2014;5:2590–601.
- [24] LUMEN, "Project Lumen," TNO; Innosyn; IMEC; Zuyd Hogeschool; Universiteit Hassel; Ecosynth, 03 April 2023. [Online]. Available: https://www.project-lumen. nl/project-lumen/.
- [25] Spotlight, "Spotlight: Sunlight production of chemical fuels," Photonics, 03 April 2023. [Online].
- [26] Xu M, den Hartog T, Cheng L, Wolfs M, Habets R, Rohlfs J, et al. ChemPhotoChem 2022;6, e202100289.
- [27] Molaeimanesh GR, Torabi F. Chapter 4 Hydrogen storage systems. In: Fuel Cell Modeling and Simulation - From Microscale to Macroscale. Tehran: Iran, Iran University of Science and Technology (IUST); 2023. p. 269–82.
- [28] NREL, "FY19-FY21 Concentrating Solar Power Systems Analysis Final Report," NREL, 2023.
- [29] BullionVault, "bullionvault," 20 10 2022. [Online]. Available: https://www.bullionvault.com/gold-price-chart.do. [Accessed 21 07 2022].
- [30] Chemanalyst, "Titanium Dioxide Price Trend and Forecast," 25 12 2022. [Online]. Available: https://www.chemanalyst.com/Pricing-data/titanium-dioxide-52. [Accessed 2023].
- [31] ASPENTech, "ASPEN Process Simulation Software," Aspen, MA, 2022.
- [32] Blok K, Nieuwlaar E. Introduction to Energy Analysis. Routledge Earthscan 2020.
- [33] IEA, Average age and typical lifetime of assets in the chemical industry, China, IEA, Paris https://www.iea.org/data-and-statistics/charts/average-age-and-typical-lifetime-of-assets-in-the-chemical-industry-china, IEA. Licence: CC BY 4.0.
- [34] Solargis, "Global Solar Atlas," Solargis, 2022. [Online]. Available: https://globalsolaratlas.info/map. [Accessed 22 12 2022].
- [35] BP, "2021 at a glance Energy demand and emissions bounced back to around prepandemic levels in 2021, reversing the temporary reduction in 2020 resulting from the COVID-19 pandemic.," 2022. [Online]. Available: https://www.bp.com/ content/dam/bp/business-sites/en/global/corporate/pdfs/energy-economics/ statistical-review/bp-stats-review-2022-at-a-glance.pdf. [Accessed 17 01 2023].
- [36] Methanol Institute, "METHANOL PRICE AND SUPPLY/DEMAND," 2022. [Online]. Available: https://www.methanol.org/methanol-price-supply-demand/. [Accessed 17 01 2023].
- [37] Afzal S, Sengupta D, Sarkar A, El-Halwagi M, Elbashir N. Optimization approach to the reduction of CO2 emissions for syngas production involving dry reforming. ACS Sustain. Chem. 2018;7532–44.
- [38] STATISTA, "Daily European Union Emission Trading System (EU-ETS) carbon pricing from January 2022 to July 2023," STATISTA, 2023. [Online]. Available: https://www.statista.com/statistics/1322214/carbon-prices-european-union-emission-trading-scheme/#:~:text=The%20price%20ef%20emissions% 20allowances,reform%20of%20the%20EU%20eTS.. [Accessed 10 2023].
- [39] Young, et al. The cost of direct air capture and storage can be reduced via strategic deployment but is unlikely to fall below stated cost targets. One Earth 2023;6: 899–917.